"Pipe Organ" Inspired Air-Coupled Ultrasonic Transducers With Broader Bandwidth

Botong Zhu, *Student Member, IEEE*, Benjamin P. Tiller, Alan J. Walker, A. J. Mulholland, and James F. C. Windmill, *Senior Member, IEEE*

***Abstract*— Piezoelectric micromachined ultrasonic transducers (PMUTs) are used to receive and transmit ultrasonic signals in industrial and biomedical applications. This type of transducer can be miniaturized and integrated with electronic systems since each element is small and the power requirements are low. The bandwidth of the PMUT may be narrow in some conventional designs; however, it is possible to apply modified structures to enhance this. This paper presents a methodology for improving the bandwidth of air-coupled PMUTs without sensitivity loss by connecting a number of resonating pipes of various lengths to a cavity. A prototype piezoelectric diaphragm ultrasonic transducer is presented to prove the theory. This novel device was fabricated by additive manufacturing (3-D printing), and consists of a polyvinylidene fluoride thin film over a stereolithography designed backplate. The backplate design is inspired by a pipe organ musical instrument, where the resonant frequency (pitch) of each pipe is mainly determined by its length. The −6-dB bandwidth of the "pipe organ" air-coupled transducer is 55.7% and 58.5% in transmitting and receiving modes, respectively, which is ∼5 times wider than a custom-built standard device.**

***Index Terms*— 3-D print, additive manufacture, air-coupled ultrasound, broad bandwidth, piezoelectric diaphragm ultrasonic transducer, polyvinylidene fluoride (PVDF).**

I. Introduction

HIGHER resolution is the one of the most important requirements in nondestructive evaluation (NDE), biomedical imaging, and underwater sonar [1]. A broad bandwidth ultrasonic probe can achieve this requirement because the pulsewidth in the time domain is shorter when the bandwidth is wider. Piezoelectric composite transducers can have wide bandwidths by optimizing their electrical and mechanical properties [1], [2]. However, the composite transducer has much better performance in water compared to air because the acoustic impedance of the composite piezoelectric material is closer to that of water. A solution to this is to add matching layers or damping materials to broaden the frequency response around resonances [2]. However, this will also decrease the device's sensitivity. Whereas the piezoelectric transducers use thickness mode resonances, the micromachined ultrasonic transducers (MUTs) have a thin flexible film to transmit and receive ultrasound. MUTs have better performance in air because the flexible film is easier to couple with the media, with a more closely matched mechanical impedance. Further, as the film stores much less kinetic energy than bulk piezoceramic, the MUTs have larger bandwidths when in resonance [2]. The MUTs' family includes piezoelectric MUTs (PMUTs) and capacitive MUTs (CMUTs). Both of these device designs have the same flexure thin film and rigid backplate structure as shown in Fig. 1(a). The flexure vibrations of CMUTs are caused by an electrostatic force generated from an electric field between the conducting backplate and metalized film. The deflection of the PMUTs' membrane is caused by lateral strain generated from the piezoelectric effect of its piezoelectric layer [3]. Different vibration mechanism provides PMUTs with a larger transmission sensitivity, and furthermore no bias voltage is required [3], [4]. However, the bandwidths of conventional PMUTs are narrow [3]–[5], thus making them unsuitable for wide bandwidth applications [6], [7]. A PMUT's bandwidth can be broadened by applying some modified structures [3], [8], such as overlapping and arranging the frequency spectrum of membranes of different sizes and shapes [9], or using rectangular membranes [6].

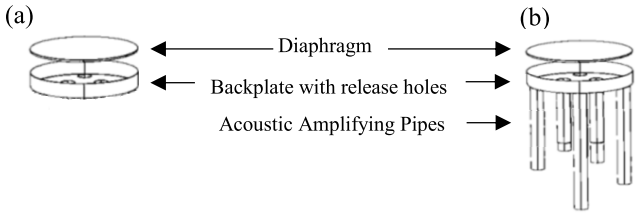

Fig. 1. (a) Conventional MUT. (b) Pipe organ piezoelectric diaphragm ultrasonic transducer.

The pipe organ backplate proposed in this paper is a novel design that can improve the bandwidth of air-coupled PMUTs without sensitivity loss or increase of active area. The concept and the mathematical model was proposed by Walker and Mulholland [10], [12] and Walker *et al.* [11] and the principle was validated via prototyping [13], [14].

Section II describes the theoretical background of the pipe organ backplate. Section III uses an FEA model to simulate the device and explain the resonant frequencies created from the

Manuscript received May 9, 2018; accepted July 17, 2018. Date of publication July 31, 2018; date of current version October 3, 2018. This work was supported in part by the Engineering and Physical Sciences Research Council under Grant EP/L022125/1 and in part by the European Research Council through the European Union's Seventh Framework Program under Grant P/2007-2013 and ERC Grant 615030. *(Corresponding author: Botong Zhu.)*

B. Zhu, B. P. Tiller, and J. F. C. Windmill are with the Centre for Ultrasonic Engineering, Electronic and Electrical Engineering Department, University of Strathclyde, Glasgow G1 1XW, U.K. (e-mail: botong.zhu@strath.ac.uk; benjamin.tiller@strath.ac.uk; james.windmill@strath.ac.uk).

A. J. Walker is with the School of Science and Sport, University of the West of Scotland, Paisley PA1 2BE, U.K. (e-mail: Alan.Walker@uws.ac.uk).

A. J. Mulholland is with the Department of Mathematics and statistics, University of Strathclyde, Glasgow G1 1XH, U.K. (e-mail: anthony.mulholland@strath.ac.uk).

Digital Object Identifier 10.1109/TUFFC.2018.2861575

backplate. Section IV introduces the manufacturing technique for the stereolithography pipe organ backplate, an improved resin formula, and the rest of the fabrication steps of the prototypes using the stereolithography backplate and commercial polyvinylidene fluoride (PVDF) thin film. Section V shows the experiment results of the prototypes, and Section VI discusses and concludes this paper.

II. Theoretical Background

A PMUT utilizes a piezoelectric layer on the top of a silicon membrane and operates in a flexural mode. After applying an electrical field to the thin plate, the lateral strain in its thickness direction makes the structure bend [15]. The vibrating membrane compresses the air and produces ultrasound. In contrast, the received ultrasound wave vibrates the film which causes charge migration between the two electrodes on the piezoelectric layer, which then can be detected by a receiving circuit [15]. The intrinsic stress of the thin plate is the factor that can dominate the resonant frequency of transducer. When the transducer has an edge-clamped film with low intrinsic stress, the resonant frequency of the circular thin plate (f_{tp}) can be estimated in (1) and (2) [3], where n is the number of the resonance mode, R is the radius of the thin plate, D_E is the flexural rigidity of the circular thin plate, h is the height of the cavity, ρ is the density of the thin plate, E is the Young's modulus, and μ is the Poisson ratio. The squeeze film effect occurs when the air gap (depth of cavity) is very narrow [16]. Squeeze film damping becomes more important than the drag force damping of air if the thickness of the gas film is smaller than one-third of the width of the plate [16]. However, this effect can be ignored in the pipe organ design presented here because the air gap is four times higher than the thickness of the thin plate. Moreover, the change of the gap depth introduced by the vibration of the thin plate is always less than 1% of the depth of the gap

$$f_{\text{tp}} = \frac{n}{2\pi R^2}\sqrt{\frac{D_E}{\rho h}} \tag{1}$$

$$D_E = \frac{Eh^3}{12(1-\mu^2)}. \tag{2}$$

A pipe organ produces sound by driving pressurized air into each individual pipe via the keyboard and pump system. The shape of individual pipes affects the sound produced; however, the resonant frequencies of the pipes are mainly determined by the length of the pipes and the velocity of sound [12]. The resonant frequency can be calculated by the theory of pipes [13] which states that the fundamental resonant frequency of an open pipe (both ends open) occurs when the length of pipe is equal to $\lambda/2$, where λ is the wavelength of sound, and the fundamental resonant frequency of a closed pipe (one end is closed and the other end is open) occurs when the length of pipe is equal to $\lambda/4$. The resonant frequency of open cylindrical pipes is given in (3), where v is the speed of sound in air, L is the length of pipe, and r is the radius of the pipe

$$f_p = \frac{nv}{2(L+1.6r)}. \tag{3}$$

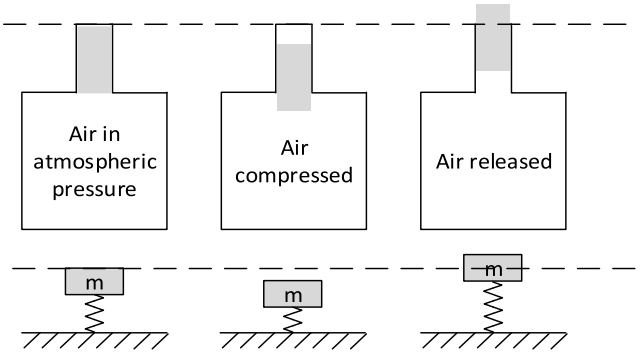

Fig. 2. Schematic of a Helmholtz Resonator.

The pipes connecting the cavity to the atmosphere enable air to flow in and out which can further reduce the effect of squeeze film damping and squeeze film resistance.

A Helmholtz resonator is an air-filled cavity with one open end. When a sound wave gives an initial force to a portion of air (depicted as the gray part in Fig. 2), the air will vibrate since the air inside the cavity acts as a spring. Therefore, the Helmholtz resonator can be regarded as a very classic spring-mass system that can support harmonic motion. In the pipe organ backplate, the pipes and cavity are formed into a Helmholtz resonator [17]. Similar to the organ pipes with different lengths and resonant frequencies, this resonator also has a resonant frequency (f_h) that can improve the sensitivity in a specific frequency range. The central frequency can be calculated in (4), where S is the total cross-sectional area of the pipe and V is the volume of the cavity

$$f_h = \frac{v}{2\pi}\sqrt{\frac{S}{VL}}. \tag{4}$$

Helmholtz resonators are well documented in many acoustic applications including acoustic energy harvesters [18], [19] and microelectromechanical system microphones [20], where they are used to enhance the sensitivity when receiving sound. The pipe organ diaphragm ultrasonic transducer proposed in this paper is based on the conventional MUT's design [as in Fig. 1(a)], but connects many acoustic amplifying pipes with different lengths to the backplate [as in Fig. 1(b)] to enhance the bandwidth in both transmitting and receiving modes. The design stage involves optimizing each pipe's length, and the cavity's size, so their resonant frequencies are close but not equal to the thin plate's resonant frequency and in so doing the overall bandwidth is increased. Moreover, the pipe-organ inspired resonator can amplify selected frequencies in receiving and transmitting ultrasound. As shown in Fig. 3, the metalized PVDF layer is clamped on the top of the backplate as an active part to produce (or receive) ultrasound and the pipe organ backplate can be thought of as a "musical instrument" which can amplify different selected frequencies (pitches) at the same time.

III. Finite-Element Modeling

Walker and Mulholland [10], [12] and Walker *et al.* [11] investigated the relationship between the number of pipes and

TABLE I
SIX DESIGNS TO ILLUSTRATE THE COUPLING EFFECT BETWEEN THE CAVITY, THE MULTIPLE PIPES, AND THE CIRCULAR MEMBRANE

Device	No pipe (I)	4 pipes (II)	4 pipes (III)	8 pipes (IV)	8 pipes (V)	13 pipes (VI)
Orientation pipe	n/a	No	No	No	Yes	Yes
Volume of cavity V (mm^3)	6.38	6.38	6.38	6.38	6.38	6.38
Depth of cavity h (mm)	0.97	0.97	0.97	0.97	1.45	1.45
Diameter of pipes d (mm)	n/a	0.424	0.6	0.424	0.424	0.424
Radius of cavity R (mm)	1.45	1.45	1.45	1.45	1.45	1.45
Length of pipes L (mm)	n/a	7.1, 6.8, 6.6, 6.4	7.1, 6.8, 6.6, 6.4	7.1, 7.0, 6.9, 6.8, 6.7, 6.6, 6.5, 6.4	7.1, 7.0, 6.9, 6.8, 6.7, 6.6, 6.5, 6.4	7.3, 7.2, 7.1, 7.0, 6.9, 6.8, 6.7, 6.6, 6.5, 6.4, 6.3, 6.2
Total area of the pipe S (mm^2)	n/a	0.56	1.13	1.13	1.13	1.68

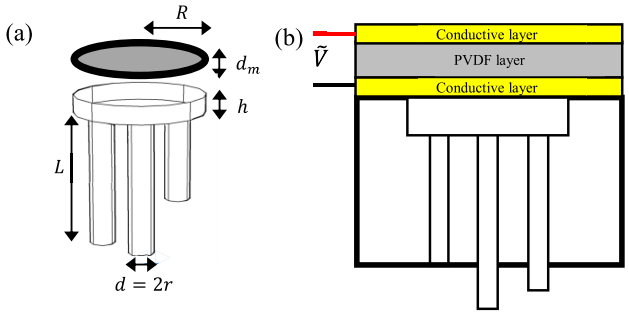

Fig. 3. (a) Parameters of the pipe organ transducer. (b) Sectional-cut plot of the backplate and the piezoelectric membrane.

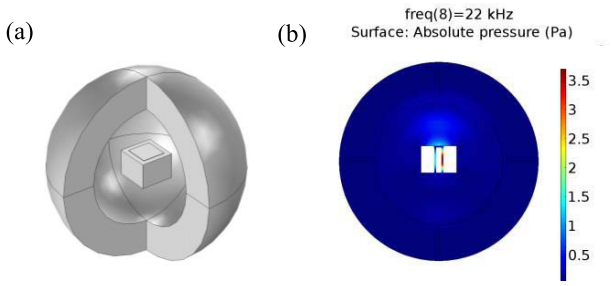

Fig. 4. (a) Schematic of the COMSOL model. (b) The x-z cut plane of a pressure plot in the cavity, pipes, and the surrounding air sphere.

the bandwidth improvement of the pipe organ transducers through 1-D mathematical models. They concluded that the bandwidth increased as the number of pipes increased, up to a perceived limit when over 80 pipes were used. In this present work, there were manufacturing constraints and so the study investigated devices with no pipes, four pipes, eight pipes, and 13 pipes emerging from the back cavity. The effect of the orientation of pipes on the performance of the transducers was also investigated.

Fig. 4(a) shows a schematic of the pipe organ transducer which was simulated by using a commercial FE software COMSOL Multiphysics (Comsol AB, Stockholm, Sweden) to optimize the design parameters. This model can calculate the resonant frequencies of the circular thin plate, pipes, and cavity accurately and also simulate the transducer in transmitting and receiving modes. The simulation model included the solid mechanics domain to simulate the mechanical vibration of both the pipe organ backplate and the PVDF film, the pressure acoustic domain to simulate the absolute pressure and coupling effect between the cavity and pipes, the electrostatics domain to simulate the charge migration inside the piezoelectric material, and finally, a multiphysics model was applied to simulate the coupled boundaries between different physical domains. An air sphere was defined to enclose the transducer to simulate its working environment. The boundary layer of the air sphere was defined as a perfectly matching layer to make sure that sound waves can pass through the boundary without reflection, as shown in Fig. 4(b). Viscous damping was added to the air domains to make the model more realistic. Acoustic wave excitation (electric signals) was introduced to vibrate the thin film to simulate the receiving or transmitting modes of the transducer. Finally, a frequency domain simulation evaluated the system from 15 to 70 kHz with a 0.5-kHz sampling rate.

Sections III-A and III-B investigate the resonant frequency and amplitude of the circular membrane, cavity, and pipes when changing the pipe's number and orientation. Section III-C (Table II) provides the parameters of three optimized samples which can be used in practical manufacturing.

A. Investigating the Resonance of the Cavity and Pipes

The relationship between the parameters of the pipes and the absolute pressure level inside the cavity of the transducer was investigated with the COMSOL model described above. The absolute pressure level inside the cavity directly correlates with the vibration and the electric potential of the piezoelectric thin plate [19]. There are four designs (as shown in Table I) which have different sizes or numbers of pipes for comparison: no-pipe device (I), four-pipe devices with different pipe diameters (II) and (III), and eight-pipe device (IV). The simulated frequency spectrum is given in Fig. 6, and the related pressure and displacements plot are given in Fig. 5. The dashed boxes in Fig. 6 from left to right represent: (a) the fundamental mode of the Helmholtz resonator, (b) the fundamental mode of the pipes, (c) the second harmonic mode of the Helmholtz resonator, (d) the fundamental mode of the circular thin plate, (e) the second harmonic mode of pipes, and (f) the third harmonic mode

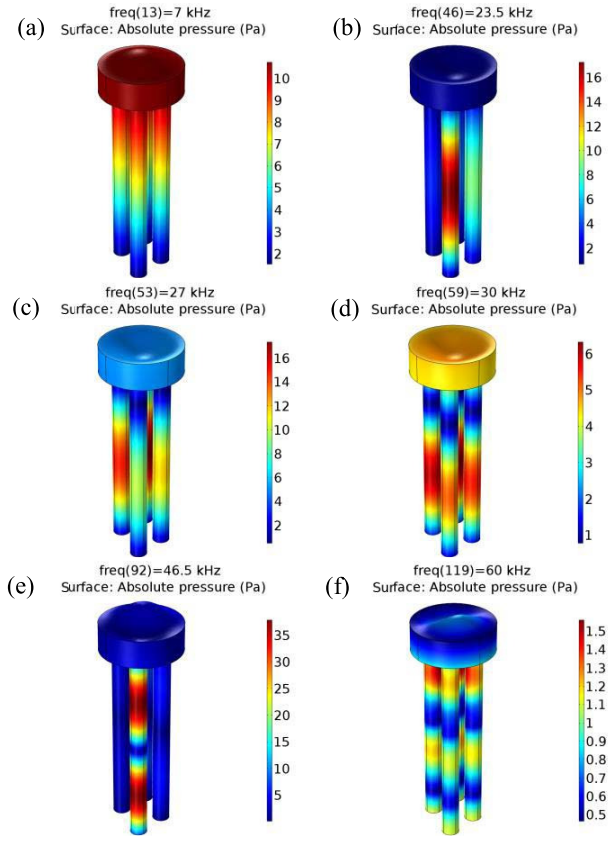

Fig. 5. The pressure (different resonances) in the pipes and cavity and the vibration of the thin plate when frequency is (a) 7kHz, (b) 23.5 kHz, (c) 27 kHz, (d) 30 kHz, (e) 46.5 kHz, and (f) 60 kHz for the 4 pipes device (III), with (a)–(f) corresponding to the frequency in Fig. 6.

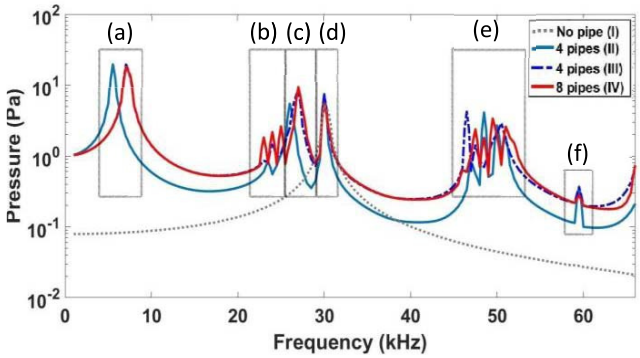

Fig. 6. Absolute pressure in the cavity against frequency to investigate the number and length of pipes. (a) Fundamental mode of the Helmholtz resonator. (b) Fundamental mode of the pipes. (c) Second harmonic mode of the Helmholtz resonator. (d) Fundamental mode of the circular thin plate. (e) Second harmonic mode of pipes. (f) Third harmonic mode of the Helmholtz resonance.

of the Helmholtz resonance, respectively. Three conclusions can be obtained from Fig. 6:

1) Designs III and IV have the same first (a) and second (c) Helmholtz resonance because their cross-sectional area, volume of cavity, and the average pipe length are equal [as shown in (4)].
2) Design IV has more frequency spectrum fluctuations in area (b) than designs II and III because it has more pipes.
3) All of the pipe organ designs (II, III, IV) have larger gain than the reference no-pipe device (I) because the Helmholtz resonance can improve the overall sensitivity.

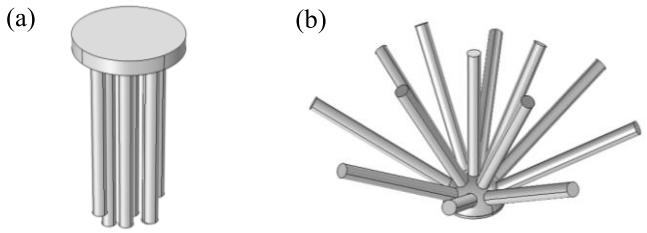

Fig. 7. Air domain of the pipe organ backplate (a) without and (b) with pipe orientation.

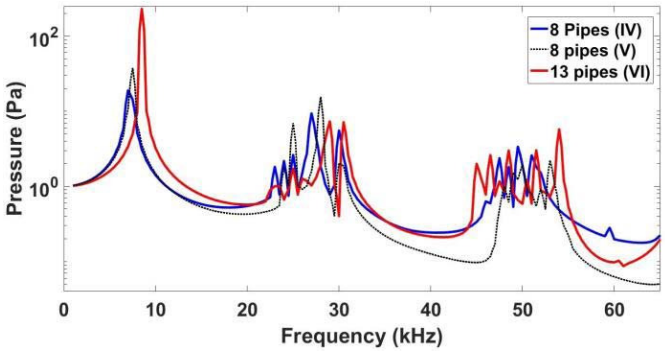

Fig. 8. Absolute pressure in the cavity against frequency to investigate the orientation of pipes.

B. Investigating the Orientation of the Pipes

A further improved pipe organ backplate design was proposed in order to increase the number of pipes [as in Fig. 7(b)] with the same fabrication resolution, which was called the "hedgehog" design. The half-sphere cavity gives a larger surface area to accommodate more pipes and also helps the ultrasonic energy focus to the center of the thin plate. In this section, there are three designs (as shown in Table I) for comparison: eight pipes without orientation (IV), eight pipes with orientation (V), and 13 pipes with orientation (VI). Two conclusions can be obtained from Fig. 8.

1) The "hedgehog" 13-pipes device (VI) provides the greatest Helmholtz resonance pressure, which is around 7 kHz, and the "hedgehog" eight-pipes device (V) has larger resonance pressure than the vertical eight-pipes device (IV).
2) The 13-pipes "hedgehog" device (VI) gives more frequency spectra fluctuations in the pipes' second harmonics than the other two devices around 50 kHz.

C. Optimized Samples

The parameters given in Table I were only used to study and quantify the resonant frequencies of the pipe organ backplate. The resonances are far away from each other in order to locate individual ones clearly. In a practical design, the resonances should be much closer to each other in order to provide more stable gain in a specific frequency range. This section provides two optimized pipe organ (vertical and hedgehog pipes) designs to compare against the standard device (as in Table II).

TABLE II
THREE OPTIMIZED SAMPLES IN PRACTICAL MANUFACTURING

Device	13 pipes	8 pipes	No pipe
Orientation pipe	Yes	No	n/a
Depth of cavity h (mm)	1.45 (half-sphere)	0.4	0.4
Diameter of pipes d (mm)	0.424	0.424	n/a
Radius of thin plate R (mm)	1.45	1.45	1.45
Length of pipes L (mm)	5.1, 5.1, 5.2, 5.3, 5.4, 5.5, 6.2, 5.5, 6.0, 6.6, 6.7, 6.9, 7.0	7.9, 7.9, 7.8, 7.7, 7.6, 7.4, 7.2, 7.2	n/a
Overall Size (mm^2)	126.7	50.2	2.46

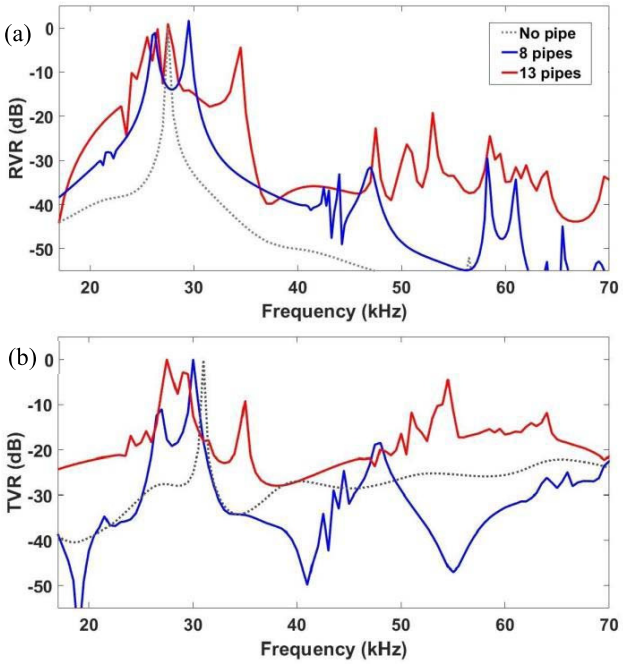

Fig. 9. Simulated normalized (a) receiving voltage response (RVR) and (b) transmitting voltage response (TVR).

The extra overall size of this pipe organ transducers arise from the length of the pipes. The active areas (piezoelectric thin plate) are the same. With ongoing developments in manufacturing resolution, it is possible to miniaturize the whole device to increase the central frequency. The normalized transmitting voltage response (TVR) and receiving voltage response (RVR) are shown in Fig. 9. The no-pipe device has a very narrow bandwidth at 29 kHz, whereas the pipe organ devices have many small peaks at around 30 kHz and 55 kHz. In other words, the pipe organ transducers should have larger operating frequency ranges (wider bandwidth), which matches the 1-D theoretical conclusions made by Walker and Mulholland [12]. This model only includes the air damping (but not the material damping) which makes the amplitude infinitely large at resonant frequency. Manually adding a material damping does improve the simulation result, but it will take away the possibility of easily locating different resonant frequencies in the design stage. Therefore, the bandwidth of the transducers is not compared in the simulation section of this paper, but will be in the experimental section.

Fig. 10. £1 coin and stereolithography pipe organ backplates for scale.

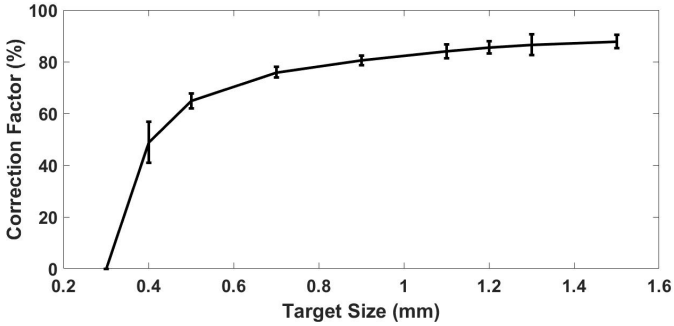

Fig. 11. Correction factor against target diameter. The error bar was from five measurements.

IV. FABRICATION

A. Stereolithography Backplates

After building a CAD model, an Asiga Pico Plus 27 additive manufacturing machine was utilized to fabricate the pipe organ backplate (see Fig. 10). This is a commercial stereolithography 3-D printer with 27-μm pixel resolution in the xy plane and $\sim 1\mu m$ in z-resolution. However, the actual print resolution is worse than this as it also depends on many other factors such as the constituents of the printer resin and the exposure time for each layer, among other things. Instead of using commercial resins directly, the improved resins [21] used in this project are prepared by mixing polyethylene (glycol) diacrylate with molecular weight of 250 along with (2-, 4-, 6-trimethylbenzoyl) phenylphosphane oxide (Irgacure 819) (1% by weight) and Sudan I (0.2% by weight) vigorously in a spinner. Gong *et al.* [21] proposed that the resins formed by this improved formula will present long-term stability in water and higher printing resolution. The exposure time is set to be 2 s with a 10-μm build layer.

During manufacture, the actual printed size was found to always be smaller than the target size because of polymer shrinkage [22]. So a correction factor was required to compensate for this. First of all, calibration pipes were printed with different lengths and diameters. Second, a high-resolution optical microscope system was used to measure the radii. The mean value between five measurements was then calculated. Finally, the correction factor was calculated from (5) and the data plotted in Fig. 11, with an error bar to show that when the diameter is less than 0.5 mm, the correction factor dramatically decreases. In other words, a ~0.5-mm diameter pipe is the smallest diameter that can be fabricated with this technology.

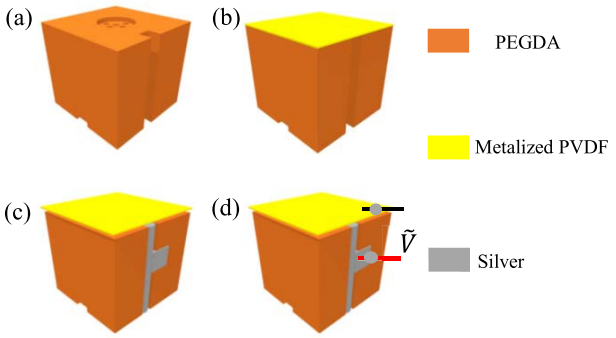

Fig. 12. Four steps fabricate the pipe organ transducer. (a) Stereolithography pipe organ backplate. (b) Gluing metalized PVDF thin film. (c) Silver paint the gap. (d) Connect copper wire to the electrode.

In order to connect more pipes to the cavity, the diameter of the pipes should be as small as possible. This is the reason why $d = 0.48$ mm is chosen for this work

$$\text{Correction factor} = \frac{\text{Actual Diameters}}{\text{Target Diameters}}. \tag{5}$$

B. PVDF Thin Film and Circuit

Fig. 12 shows a schematic illustrating the further four steps of the fabrication. The manufacture starts with (a) the additive manufactured pipe organ backplate with a gap on the side; (b) two-side-metalized PVDF film (Precision Acoustics Ltd, Dorset, U.K.) is attached on the top backplate with superglue; (c) the gap is filled with silver paint to connect the bottom surface of PVDF thin film. Finally, (d) a copper wire is connected to the silver gap and another one to the top surface of the film. When attaching the PVDF film with superglue, some of the superglue may enter the cavity which makes the diameter smaller (or larger) than the designed size, and thus changes the resonance of the thin plate's flexure mode.

V. Experimental Setup and Results

The evaluation of the pipe organ ultrasonic transducer includes measuring the vibration of the active film and the electrical signal in both time and frequency domains.

A. 3-D Laser Doppler Vibrometer

Initially, 10-V wideband periodic chirps with equal energy across frequencies from 15 to 70 kHz were generated by a signal generator to drive the active film into vibration. Second, the front face average displacement was obtained by a 3-D LDV (MSA100-3D, Polytec, Inc., Waldbronn, Germany). Finally, the frequency spectrum and the vibration modes of the resonant frequencies were shown (see Fig. 13). From this test, the fundamental and second harmonic flexure modes of the circular PVDF film between the three devices (as in Table II) were 29 ± 3 and 58 ± 6 kHz, respectively (which are the same as the theoretical prediction).

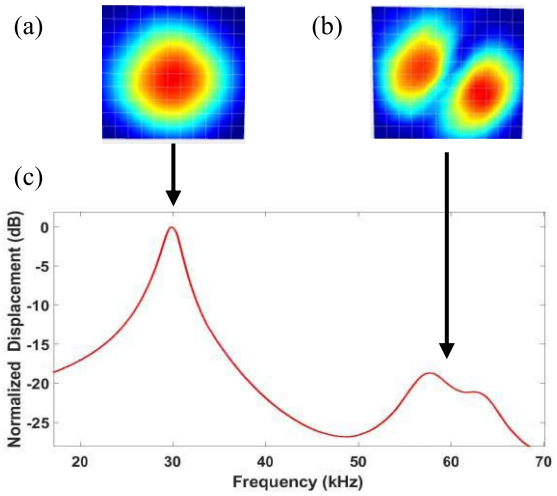

Fig. 13. (a) Fundamental, (b) 2nd harmonic flexure mode of the circular PVDF film and the colors represent the displacement in the out of plane direction and (c) average displacement spectrum of the active area measured by 3-D LDV.

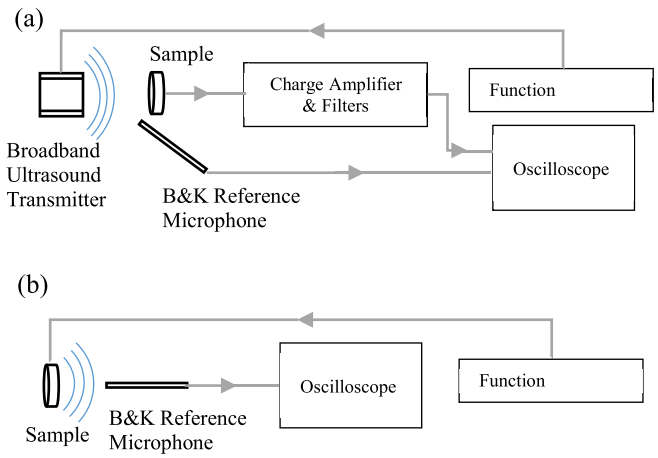

Fig. 14. Simplified schematic of the experimental setup of the receiving and transmitting modes.

B. Electrical Signal Measurement

The experimental setup for measuring the receiving and transmitting bandwidth is shown in Fig. 14(a) and (b), respectively. In Fig. 14(a), the function generator produced a 70-kHz pulse which has equal energy up to ~70 kHz to drive a broadband ultrasonic transmitter (Ultra Sound Advice Loudspeaker). The sample was far enough away from the transmitter to avoid near-field effects. The electrical signal generated from the sample was amplified by a commercial charge amplifier (Brüel and Kjær type 2692) with a custom-built filter (bandwidth 10–100 kHz) system, and finally acquired on an oscilloscope. A 1/8 in reference microphone (Brüel and Kjær, Type 4138) was used to measure the reference sound pressure around the sample. The frequency response of this microphone is calibrated to be flat up to 110 kHz. An amplitude correction algorithm was utilized to compensate for the transmitter's output variance. In Fig. 14(b), the function generator produced a 10-V pulse to drive the film into vibration and the ultrasound

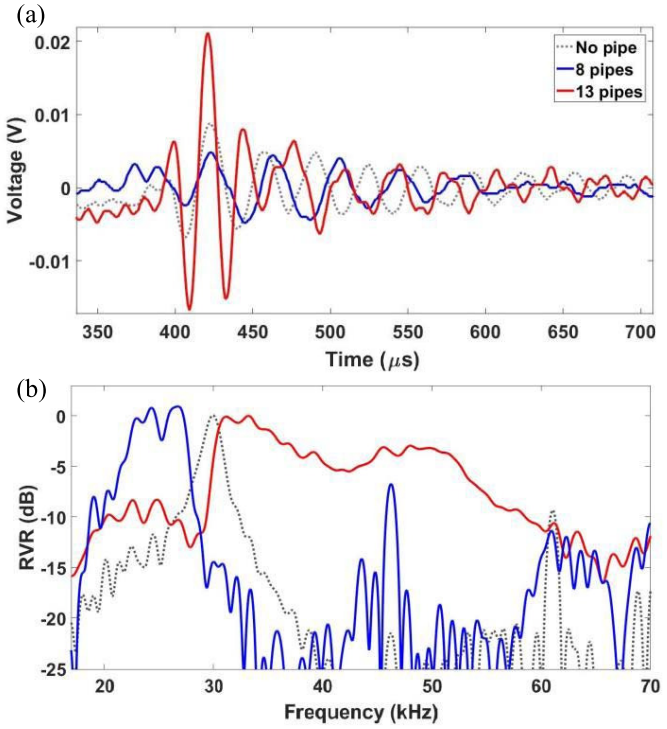

Fig. 15. Receiving voltage response (RVR) in (a) time domain and (b) frequency domain.

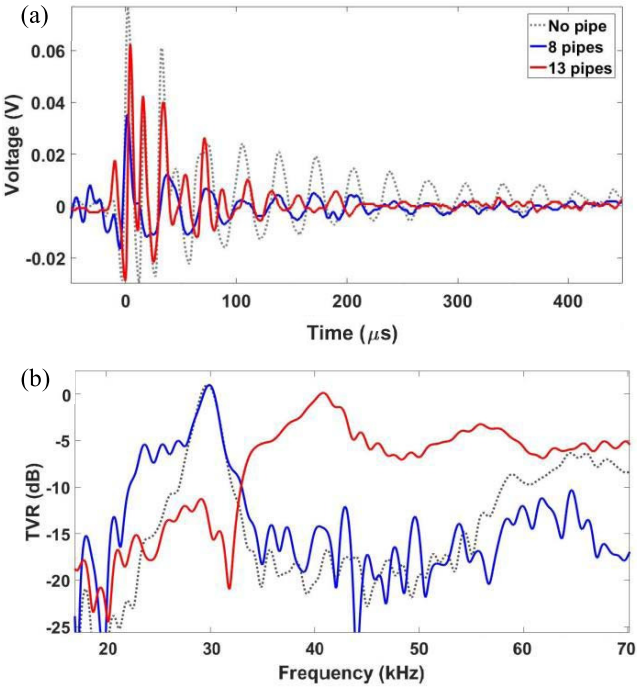

Fig. 16. Transmitting voltage response (TVR) in (a) time domain and (b) frequency domain.

field generated by the sample was measured by the reference microphone directly. Since the frequency range of our device is narrower than 110 kHz, no amplitude compensation is required. Figs. 15 and 16 show the electrical signal response in TVR and RVR between the standard no-pipe, eight-pipe, and "hedgehog" 13-pipe devices.

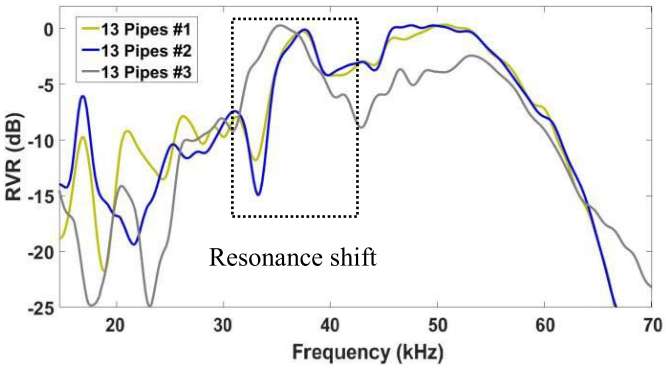

Fig. 17. Repeatability experiment of three 13-pipes pipe organ transducers in RVR measurement.

TABLE III
EXPERIMENTAL RESULT OF TVR AND RVR

Mode	Device	13 pipes	8 pipes	No pipe
TVR	-6 dB Bandwidth	55.7%	29.2%	12.3%
	Signal strength	0.091V	0.048V	0.106V
	Central frequency	47 kHz	27kHz	29kHz
	20% Peak-Peak Pulse length	8.8μs	20.1μs	20.5μs
RVR	-6 dB Bandwidth	58.5 %	26.0 %	9.7 %
	Signal strength	0.037 V	0.010V	0.015V
	Central frequency	41kHz	26kHz	30kHz
	20% Peak-Peak Pulse length	12.3μs	20.6μs	27μs

C. Repeatability Experiment

In order to prove the repeatability of the "hedgehog" 13-pipe transducer, another three samples were fabricated in order to remeasure their RVR (see Fig. 17). The −6-dB bandwidth of those three devices are 52.9% (not a continuous bandwidth), 50.9%, and 50.9%, respectively, which are very close to the first 13-pipes device in Table III (58.5%). Moreover, their frequency spectrums are also very similar (above 25 kHz) except one of the resonances was shifted at around 37 kHz. This was caused by the tolerance of fabrication when manually attaching the PVDF film with superglue.

VI. DISCUSSION AND CONCLUSION

A. Simulation and Experimental Result Discussion

The pipe organ backplate is a resonator which is formed by a cavity with connecting of pipes of various lengths. Therefore, it includes many fundamental resonances and harmonics from those components. Sections II and III evaluated those resonant frequencies from both mathematical and FEA model aspects to give the same conclusions. Section III-A investigated the resonance of the pipes and the cavity. The simulation results, shown in Fig. 6, indicate that the resonant frequency of a pipe is mainly determined by its length, which can also be explained by (3). Furthermore, (4) indicates that the resonant frequency of the Helmholtz resonator depends on the area of the opening and the cavity volume. Therefore, samples III and IV have the same Helmholtz resonant frequency in Fig. 6 boxes

(a) and (c). Section III-B investigated the effect of the orientation of the pipes ("hedgehog" design). The pipes are designed to be orientated at different angles since previous 1-D theoretical work concluded that the number of pipes should be as high as possible in order to have the widest bandwidth [12]. However, the number of pipes is limited by the resolution of the additive manufacturing technique in the laboratory. The "hedgehog" design provides a larger space to arrange the pipes because of the curved cavity surface. In other words, the "hedgehog" design increases the number of pipes with the same manufacturing resolution. Moreover, the "hedgehog" design provides additional benefits and Figs. 8 and 9 show that the "hedgehog" design has a larger Helmholtz resonance and more stable gain, because the orientated pipes can focus ultrasound energy to the thin plate center.

In the optimized designs, the resonant frequencies of the cavity, multiple pipes, and the circular piezoelectric film were chosen to be close to each other in order to have a flat bandwidth response in both TVR and RVR. The results in Table III show that the bandwidth of the pipe organ devices is at least twice as wide as that of the no-pipe device with comparable sensitivity. The "hedgehog" device has the largest bandwidth and shortest pulselength in both transmitting and receiving modes. However, the disadvantage is that the "hedgehog" device also requires larger space to place the orientated pipes. The result from the 3-D LDV (as shown in Fig. 13) indicates that the first flexure mode of those three transducers is around 29 kHz, which is the same as the FEA result and the value calculated from (1) and (2). The FEA simulation result has sharp gain peaks which caused the simulated bandwidth to be smaller than the experimental bandwidth. This is because the model did not include any electrical or mechanical damping. However, the resonant frequencies from different components of the pipe organ backplate are a good match. The pipes' fundamental and second harmonic resonance varied from 20 to 25 kHz and 45 to 55 kHz, respectively, and the Helmholtz resonance was located at 35 kHz to fill the gap between the pipes' resonance modes and increase the overall device sensitivity. This is why the 13-pipes pipe organ transducer can introduce a stable gain from 30 to 55 kHz in the experiment results. Although the vertical pipe design can have similar pipe lengths and cavity size, the "hedgehog" device can focus the ultrasound energy to the middle of the thin plate. Therefore, the "hedgehog" device has larger sensitivity improvement in the pipes' resonant frequencies. The repeatability experiment proved that the fabrication and the measurement stages are repeatable. All of the potential errors are from the tolerance of the fabrication.

B. Conclusion

The bandwidth of conventional PMUTs is too narrow to be used in wide-bandwidth applications [7]. This paper presented a novel backplate design (resonator) to improve the bandwidth by selecting and enhancing the frequency range of interest. The frequency range can be carefully controlled through the specific parameters of the backplate. The principles were studied via mathematical equations and FEA models. The models indicated that the pipe organ backplate introduced Helmholtz resonances and multiple pipes' resonances to the circular thin plate's resonance to increase the device bandwidth without sensitivity loss. This also provided several conclusions to locate and quantify different types of resonances in the frequency domain. Two optimized designs were selected for the fabrication stage to compare against the custom-built standard device. An additive manufacturing technique for the pipe organ backplate is introduced. It is a faster prototyping method for fabricating piezoelectric diaphragm ultrasonic transducers. An improved resin formula was used to increase the manufacture resolution of the backplate. Finally, two experiments were designed to evaluate the response of two pipe organ transducers, and a standard transducer, in both TVR and RVR. The -6-dB bandwidth of the "hedgehog" 13-pipes device was found to be up to 58.5% in RVR, which was 2.25 times larger than the vertical eight-pipe device, and 6 times larger than the custom-built standard device. In the TVR, the -6-dB bandwidth of the "hedgehog" 13-pipes device was up to 55.7%, which was 1.9 times larger than the eight-pipes device, and 4.6 times larger than the customer-built standard device. The repeatability experiment shows that the fabrication and measurement progress are repeatable. The error originated from the manual fabrication process. With the ongoing development of additive manufacturing, some researchers [23] claim that they can use TPP for fabrication of 3-D structures with a lateral resolution below 200 nm. The authors latest simulation results suggest that the overall size of the pipe organ air-coupled transducer can be miniaturized to be ~ 500 μm, which will result in an operating frequency of 480 kHz, which is more applicable to applications such as NDE. Furthermore, it is possible to imagine that the fabrication could be achieved directly on a piezoelectric film to order to replace the gluing process used for this paper's prototypes.

ACKNOWLEDGMENT

The authors would like to thank Y. Zhang for designing and fabricating the custom-built filters for measuring the electrical signal. They would also like to thank other staff and researchers at the Centre for Ultrasonic Engineering, University of Strathclyde, Glasgow, U.K., for their support throughout this research work. Data set available: http://dx.doi.org/10.15129/fa341875-f1b1-4bfd-b052-41b965de95c4

REFERENCES

[1] H. Fang, Z. Qiu, R. L. O'Leary, A. Gachagan, and A. J. Mulholland, "Improving the operational bandwidth of a 1–3 piezoelectric composite transducer using Sierpinski Gasket fractal geometry," in *Proc. IEEE Int. Ultrason. Symp. (IUS)*, Nov. 2016, pp. 8–11.

[2] P. C. Eccardt and K. Niederer, "Micromachined ultrasound transducers with improved coupling factors from a CMOS compatible process," *Ultrasonics*, vol. 38, nos. 1–8, pp. 774–780, 2000.

[3] Y. Qiu *et al.*, "Piezoelectric micromachined ultrasound transducer (PMUT) arrays for integrated sensing, actuation and imaging," *Sensors*, vol. 15, no. 4, pp. 8020–8041, 2015.

[4] D. E. Dausch, J. B. Castellucci, D. R. Chou, and O. T. von Ramm, "Theory and operation of 2-D array piezoelectric micromachined ultrasound transducers," *IEEE Trans. Ultrason., Ferroelectr., Freq. Control*, vol. 55, no. 11, pp. 2484–2492, Nov. 2008.

[5] A. Guedes, S. Shelton, R. Przybyla, I. Izyumin, B. Boser, and D. A. Horsley, "Aluminum nitride pMUT based on a flexurally-suspended membrane," in *Proc. 16th Int. Solid-State Sens., Actuators Microsyst. Conf. TRANSDUCERS*, Jun. 2011, pp. 2062–2065.
[6] T. Wang, T. Kobayashi, and C. Lee, "Micromachined piezoelectric ultrasonic transducer with ultra-wide frequency bandwidth," *Appl. Phys. Lett.*, vol. 106, no. 1, p. 013501, 2015.
[7] P. Muralt *et al.*, "Piezoelectric micromachined ultrasonic transducers based on PZT thin films," *IEEE Trans. Ultrason., Ferroelectr., Freq. Control*, vol. 52, no. 12, pp. 2276–2288, Dec. 2005.
[8] T. Wang, R. Sawada, and C. Lee, "A piezoelectric micromachined ultrasonic transducer using piston-like membrane motion," *IEEE Electron Device Lett.*, vol. 36, no. 9, pp. 957–959, Sep. 2015.
[9] A. Hajati *et al.*, "Monolithic ultrasonic integrated circuits based on micromachined semi-ellipsoidal piezoelectric domes," *Appl. Phys. Lett.*, vol. 103, no. 20, p. 202906, 2013.
[10] A. J. Walker and A. J. Mulholland, "A theoretical model of an electrostatic ultrasonic transducer incorporating resonating conduits," *IMA J. Appl. Math.*, vol. 75, no. 5, pp. 796–810, 2010.
[11] A. J. Walker, A. J. Mulholland, E. Campbell, and G. Hayward, "A theoretical model of a new electrostatic transducer incorporating fluidic amplification," in *Proc. IEEE Ultrason. Symp.*, Nov. 2008, pp. 1409–1412.
[12] A. J. Walker and A. J. Mulholland, "A pipe organ-inspired ultrasonic transducer," *IMA J. Appl. Math.*, vol. 82, no. 6, pp. 1135–1150, 2017.
[13] E. Campbell, W. Galbraith, and G. Hayward, "A new electrostatic transducer incorporating fluidic amplification," in *Proc. IEEE Ultrason. Symp.*, Oct. 2006, pp. 1445–1448.
[14] B. Zhu, B. Tiller, A. Walker, A. Mulholland, and J. Windmill, "'Pipe organ' air-coupled broad bandwidth transducer," in *Proc. IEEE Int. Ultrason. Symp. (IUS)*, Sep. 2017, pp. 6–9.
[15] F. Akasheh, T. Myers, J. D. Fraser, S. Bose, and A. Bandyopadhyay, "Development of piezoelectric micromachined ultrasonic transducers," *Sens. Actuators A, Phys.*, vol. 111, nos. 2–3, pp. 275–287, 2004.
[16] M. Bao and H. Yang, "Squeeze film air damping in MEMS," *Sens. Actuators A, Phys.*, vol. 136, no. 1, pp. 3–27, 2007.
[17] J. E. Mclennan and J. Close, "A0 and A1 studies on the violin using CO_2, he, and air/helium mixtures," *Acta Acust.*, vol. 89, no. 1, pp. 176–180, Apr. 2002.
[18] S. B. Horowitz, M. Sheplak, L. N. Cattafesta, III, and T. Nishida, "A MEMS acoustic energy harvester," *J. Micromech. Microeng.*, vol. 16, no. 9, p. S174, 2006.
[19] R. A. Rahim and M. J. B. Johari, "Design and simulation of MEMS helmholtz resonator for acoustic energy harvester," in *Proc. Int. Conf. Comput. Commun. Eng. (ICCCE)*, Jul. 2016, pp. 505–510.
[20] H. Takahashi, A. Suzuki, E. Iwase, K. Matsumoto, and I. Shimoyama, "MEMS microphone with a micro Helmholtz resonator," *J. Micromech. Microeng.*, vol. 22, no. 8, p. 085019, 2012.
[21] H. Gong, M. Beauchamp, S. Perry, A. T. Woolley, and G. P. Nordin, "Optical approach to resin formulation for 3D printed microfluidics," *RSC Adv.*, vol. 5, no. 129, pp. 106621–106632, 2015.
[22] J. Stampfl *et al.*, "Photopolymers with tunable mechanical properties processed by laser-based high-resolution stereolithography," *J. Micromech. Microeng.*, vol. 18, no. 12, p. 125014, 2008.
[23] J. Serbin *et al.*, "Femtosecond laser-induced two-photon polymerization of inorganic–organic hybrid materials for applications in photonics," *Opt. Lett.*, vol. 28, no. 5, pp. 301–303, 2003.

Botong Zhu (S'17) received the bachelor's degree from the University of Strathclyde, Glasgow, U.K., in 2015, where he is currently pursuing the Ph.D. degree with the Department of Electronic and Electrical Engineering. He is also a Ph.D. student with the EPSRC Centre for Doctoral Training of Quantitative NDE, U.K.

His current research interests include air-coupled transducer development.

Benjamin P. Tiller received the M.Sc. degree in physics with theoretical physics from the University of Nottingham, Nottingham, U.K., and the Ph.D. degree from the University of Glasgow, Glasgow, U.K., with a focus on the frequency scaling relationship of acoustic streaming in microfluidic environments.

He is currently a Research Associate with the Department of Electronics and Electrical Engineering, University of Strathclyde, Glasgow. His current research interests include development of novel 3-D printed techniques that enable new sensing technologies.

Alan J. Walker received the B.Sc. (Hons.) and Ph.D. degrees in mathematics from the University of Strathclyde, Glasgow, U.K., in 2003 and 2008, respectively.

He is a Member of the Institute of Mathematics and its Applications, and a Chartered Mathematician. He joined the University of the West of Scotland, Hamilton, U.K., as a Lecturer in mathematics, in 2015. He has over 10 years of research experience in the area of ultrasonics. His current research interests include mathematical modeling of physical and biological systems.

A. J. Mulholland was born in Glasgow, U.K., in 1966. He received the B.Sc. degree (Hons.) in mathematics from the University of Glasgow, Glasgow, in 1987, the M.Sc. degree in industrial mathematics from the University of Strathclyde, Glasgow, in 1991, and the Ph.D. degree in mathematical biology from Glasgow Caledonian University, Glasgow, in 1994.

Since 1999, he has been an Academic Member of Staff with the Department of Mathematics and Statistics, University of Strathclyde, Glasgow, where he is currently a Professor and the Head of the Department. He has been with the Centre for Ultrasonic Engineering, University of Strathclyde, since 1996, and he leads the analytical modeling activities of the center. He has authored over 100 papers in applied mathematics, particularly in the modeling of ultrasonic devices and systems.

Dr. Mulholland is a fellow of the Institute of Mathematics and its Applications.

James F. C. Windmill (M'99–SM'17) received the B.Eng. degree in electronic engineering and the Ph.D. degree in magnetic microscopy from the University of Plymouth, Plymouth, U.K., in 1998 and 2002, respectively.

He joined the Centre for Ultrasonic Engineering, University of Strathclyde, Glasgow, U.K., as a Lecturer in 2008. He is currently a Professor with the Department of Electronic and Electrical Engineering, University of Strathclyde. He has over 18 years of research and development experience in the areas of sensors and hearing systems. His current research interests include biologically inspired acoustic systems, from the fundamental biology to various engineering application topics.